Biogeosciences Discuss., 10, 17819–17857, 2013
www.biogeosciences-discuss.net/10/17819/2013/
doi:10.5194/bgd-10-17819-2013

Biogeosciences Discussions
Open Access

Diversity and distribution of *amoA*-type nitrifying and *nirS*-type denitrifying microbial communities in the Yangtze River Estuary

Y. Zhang[1,2,*], **X. Xie**[1,2,*], **N. Jiao**[1,2], **S. S.-Y. Hsiao**[3], **and S.-J. Kao**[1,3]

[1]State Key Laboratory of Marine Environmental Sciences, Xiamen University, Xiamen, China
[2]Institute of Marine Microbes and Ecospheres, Xiamen University, Xiamen, China
[3]Earth System Science Program, Taiwan International Graduate Program, Research Center for Environmental Changes, Academia Sinica, Taipei, Taiwan
[*]These authors contributed equally to this work.

Received: 23 October 2013 – Accepted: 29 October 2013 – Published: 15 November 2013

Correspondence to: Y. Zhang (yaozhang@xmu.edu.cn) and N. Jiao (jiao@xmu.edu.cn)

Published by Copernicus Publications on behalf of the European Geosciences Union.

Abstract

Coupled nitrification-denitrification plays a critical role in the removal of excess nitrogen, which is chiefly caused by humans, to mitigate estuary and coastal eutrophication. Despite its obvious importance, limited information about the relationships between nitrifying and denitrifying microbial communities in estuaries, and their controlling factors have been documented. By analyzing the ammonia monooxygenase gene *amoA*, including archaeal and bacterial *amoA*, and the dissimilatory nitrite reductase gene *nirS* using clone libraries and quantitative PCR (qPCR), we investigated the nitrifying and denitrifying microbial communities in the estuary of turbid subtropical Yangtze River (YRE), the largest river in Asia. The diversity indices and rarefaction analysis revealed a quite low diversity for both β-proteobacterial and archaeal *amoA* genes, but qPCR data showed significantly higher *amoA* gene copy numbers for archaea than β-proteobacteria, suggesting that the archaea might play a dominant role in nitrification in the YRE. Compared with the *amoA* gene, a distinctly higher level of diversity but lower gene copy numbers were found for the *nirS* gene suggesting lower denitrification than nitrification potential. ^{15}N incubation experiments indicated that nitrification rates were strongly correlated with *amoA* gene abundances while denitrification rates were below detection limit. In general, the abundances of the *amoA* and *nirS* genes were significantly higher in the bottom samples than the surface ones, and in the high-turbidity river mouth, were distinctly higher in the particle-associated ($> 3\,\mu m$) than the free-living ($0.2 \sim 3\,\mu m$) communities. Notably, analysis of correlations between the gene abundances suggested potential gene-based coupling between nitrification and denitrification, especially for the particle-associated assemblages. Statistical analysis of correlations between the community structure, gene abundances and environmental variables further revealed that dissolved oxygen and total suspended material might be the key factors controlling community spatial structure and regulating nitrification and denitrification potentials in the YRE ecosystem.

BGD
10, 17819–17857, 2013

1 Introduction

Estuary channels the continuously increasing load of anthropogenic nitrogen (N) from land to the coastal and shelf marine ecosystem. During the transportation, tightly coupled nitrification-denitrification and nitrification-anammox processes mediated by microorganisms may diminish the N loading to relieve the eutrophication stress. Nitrifiers supply oxidized N for denitrification or anammox, then denitrifiers release N via the conversion of oxidized N into gaseous N forms, such as nitrogen monoxide (NO), nitrous oxide (N_2O) and nitrogen gas (N_2), and anammox bacteria release N by oxidizing ammonium with oxidized N to N_2. Coupled nitrification-denitrification is reported to possibly regulate nitrate accumulations in estuary ecosystems (Taylor and Townsend, 2010) and remove up to 50 % of external dissolved inorganic nitrogen (DIN) that enters into estuaries (Seitzinger et al., 2006), especially in the hypoxia zone. However, few studies have been devoted to understanding the relationship between nitrification and denitrification in estuaries by comparison between nitrifying and denitrifying microbial communities.

The Yangtze River, Changjiang, is the largest river in Asia in terms of volume of water discharge and length, and the third longest in the world. The Yangtze River Estuary (YRE) lies at the interface between the Asian continent and East China Sea, and its water and suspended solid discharge is $9 \times 10^{11}\,m^3\,yr^{-1}$ and $4.9 \times 10^8\,t\,yr^{-1}$, respectively (Lin and Wu, 1999). The DIN discharge from the Yangtze River to the estuary has increased by 6 × in the past 5 decades (Wang, 2006; Yan et al., 2010). The intensive application of fertilizer and erosion of agriculture soil contribute to the high turbidity and heavily imbalanced N/P ratio (often > 80 even up to 200) of the YRE. Moreover, summer hypoxia ($< 2\,mg\,L^{-1}$ of dissolved oxygen (DO) concentration) was often observed in the bottom water of YRE (Wei et al., 2007; Wang, 2009; Zhu et al., 2011; Wang et al., 2012), and its areal extent keeps expanding since 1960 (Zhu et al., 2011). Whether denitrifying bacteria and their activity can be determined in the YRE ecosystem is critical in term of mitigating the imbalanced nutrient status, meanwhile, the re-

BGD
10, 17819–17857, 2013

lation between nitrifying and denitrifying communities in such a turbid and N-replete estuary remain unexplored.

The ammonia-oxidizing archaeal (AOA) and bacterial (AOB) *amoA* gene putatively encodes α subunit of ammonia monooxygenase enzyme, which is responsible for catalyzing the oxidation of ammonia to hydroxylamine, the first and rate-limiting step of nitrification. Quantitative analysis of the *amoA* gene shows that AOA are ubiquitous and greatly outnumber AOB in many environments (Leininger et al., 2006; Wuchter et al., 2006; De Corte et al., 2009; Abell et al., 2010). However, mounting evidence also suggests that AOB *amoA* gene abundance may actually be greater than AOA in certain regions of estuaries (Santoro et al., 2008; Wankel et al., 2011). The key enzyme in the dissimilatory denitrification pathway is nitrite reductase, which catalyzes the reduction of nitrite (NO_2^-) to NO, the first step in denitrification to produce gaseous N. The *nirS* and *nirK* genes encode cytochrome cd1 and copper-containing nitrite reductase, respectively. They are functionally and physiologically equivalent, but structurally different and cannot be detected in the same strains (Coyne et al., 1989). The *nirS* gene is more widely distributed than the *nirK* gene (Zumft, 1997; Bothe et al., 2000). It is reported that nitrite reductase genes are dominated by the *nirS* but not the *nirK* types in a turbid subtropical estuary of central Queensland (Abell et al., 2010). Another study on the sediments of the River Clone Estuary (UK) shows that only the *nirS* gene is significantly expressed in microbial communities (Nogales et al., 2002).

In this study, AOA and AOB *amoA* and bacterial *nirS* genes were investigated to analyze the diversity, abundance and spatial dynamics of nitrifiers and denitrifiers and their control environmental factors in the YRE during a spring and summer cruise (April and August 2011). The goals of this research were to (1) explore the spatial and temporal variation of the *amoA* and *nirS* genes, (2) evaluate the potential coupling between the nitrifier and denitrifier communities, and (3) identify the possible key environmental factors regulating the distribution of the *amoA*-type nitrifiers and *nirS*-type denitrifiers in the YRE.

BGD
10, 17819–17857, 2013

2 Materials and methods

2.1 Study sites and sampling

A 177 km transect with five study sites (Y1 to Y5) along the salinity gradient from the YR mouth to the open water were sampled during a spring and summer cruise (7 to 18 April and 15 to 24 August 2011). A 222 km transect with six sites (YE0 to YE5) along the latitude gradient at 122.8° E longitude and a closest-to-seashore site Y0 were sampled only during the summer cruise (Fig. 1). In total, fifty samples were collected from the surface and bottom of each station, except for site YE0, where only the surface water was sampled. Water samples were collected with a SeaBird SBE 9/11 Plus CTD system. One or two liter samples for gene analysis were filtered first through 3 µm-pore-size and then 0.2 µm-pore-size polycarbonate filters (47 mm diameter, Millipore) at a pressure of < 0.03 MPa. The 3 µm-pore-size polycarbonate filters were designated as particle-associated communities and the 0.2 µm-pore-size ones were taken as free-living communities. Only the August samples were divided into size fractions of > 3 µm and 0.22–3 µm, while only the 0.22–3 µm free-living communities were sampled during the April cruise. Filtered samples were immediately frozen on board at −20 °C and transferred to −80 °C in the laboratory until further analysis.

2.2 Biogeochemical analysis

Temperature and salinity were measured using a CTD system. DO concentrations were measured using the Winkler method. Inorganic nutrients (ammonium, nitrate + nitrite, phosphate, silicate) were measured onboard using a flow injection analyzer (AA3 system and Tri-223 autoanalyzer) and standard spectrophotometric methods (Dai et al., 2011). Total suspended material (TSM) was collected by filtering 1–4 L water sample onto pre-combusted GF/F membrane (Whatman) and weighed.

BGD
10, 17819–17857, 2013

2.3 DNA extraction, PCR, cloning and sequencing

DNA was extracted using the UltraClean Soil DNA kit (MoBio, San Diego, CA, USA) following the manufacturer's instructions. Archaeal and β-proteobacterial *amoA* gene sequences were amplified using primer sets Arch-amoAF and Arch-amoAR (Francis et al., 2005) and amoA-34F and amoA-2R (Kim et al., 2008), respectively; the γ-proteobacterial *amoA* gene was not amplified successfully from these samples using primers amoA-3F and amoB-4R (Purkhold et al., 2000). The *nirS* gene fragments were amplified using primers nirS-1F and nirS-6R (Braker et al., 1998). The PCR reaction mixture for amplifying the *amoA* gene was prepared in accordance with Hu et al. (2010) and PCR conditions were applied as described by Francis et al. (2005) and Kim et al. (2008). The PCR reaction mixture (25 µL) for amplifying the *nirS* gene contained 12.5 µL of Premix Ex Taq (TakaRa, Dalian, China), 1.6 µM of each primer, 50 µg BSA and 1.5 µL template, and PCR conditions were applied as described by Oakley et al. (2007). Amplification products were purified using an agarose gel DNA purification kit (TaKaRa), ligated into the pMD18-T vector (TakaRa) and then transformed into competent cells of *Escherichia coli* DH5α. Positive clones were screened using PCR re-amplification with vector primers M13-F/M-13R and randomly selected for sequencing using an ABI model 3730 automated DNA sequence analyzer with BigDye terminator chemistry (Applied Bio Systems, Perkin-Elmer).

2.4 Phylogenetic diversity analysis

AmoA and *nirS* gene sequences were grouped into operational taxonomic units (OTUs) based on a 5 % sequence divergence cutoff (Oakley et al., 2007; Wankel et al., 2011) using the DOTUR program (Schloss and Handelsman, 2005). Rarefaction, non-parametric coverage and phylotype richness estimators (Chao 1, Shannon and Simpson) for each clone library were also calculated using DOTUR.

DNA sequences were analyzed using the BLASTN tool, and amino acid sequences were analyzed using BLASTP to aid the selection of the closest reference sequences.

BGD
10, 17819–17857, 2013

Neighbor-joining phylogenetic trees were constructed in MEGA5 using the Maximum Composite Likelihood model with DNA sequences for the *amoA* gene and the Poisson model with translated amino acid sequences for the *nirS* gene. DNA sequences with > 95 % similar identity were grouped into the same phylotype.

2.5 Quantitative PCR amplification

Abundances of the *nirS* gene and *β*-proteobacterial and archaeal *amoA* gene were quantified using the quantitative PCR (qPCR) method and a CFX 96^{TM} Real-Time System (BIO-RAD, Singapore). The *β*-proteobacterial *amoA* gene was amplified using primers amoA-1F and amoA-2R (Kim et al., 2008); the archaeal *amoA* gene was amplified using primers Arch-amoAF and Arch-amoAR (Francis et al., 2005); and the *nirS* gene was amplified using primers nirS-1F and nirS-3R (Braker et al., 1998; Huang et al., 2011). Standard curves were constructed for the *β*-proteobacterial *amoA* gene using the plasmid DNA of the most dominant genotype clone AugY3SF15 (KF362529); for the archaeal *amoA* gene using a mixture of equal amounts of the plasmid DNA of the four most dominant genotype clones AugY0SP01 (KF362930), AugY0SP03 (KF362932), AprY3BF01 (KF362819) and AugY5BP02 (KF363129); and for the *nirS* gene using a mixture of equal amounts of the plasmid DNA of the two most dominant genotype clones AprY5BF_63 (KF363544) and AprY4BF_01 (KF363527). Using 10-fold increments, the standard concentrations were adjusted from 10^7 to 10^0 gene copies μL^{-1} for the *β*-proteobacterial *amoA* and *nirS* genes, and from 10^8 to 10^1 gene copies μL^{-1} for the archaeal *amoA* gene. QPCR amplification for the *amoA* gene was carried out as described previously (Mincer et al., 2007; Hu et al., 2011). For the amplification of the *nirS* gene, the reaction mixture (25 µL) contained 12.5 µL SYBR® Premix Ex Taq™ II (TakaRa, Dalian, China), 0.5 µM of each primer and 1 µL template DNA, and qPCR thermal cycling conditions were applied as described by Huang et al. (2011). The amplification efficiencies of PCR were always between 85 and 95 % with R^2 values > 0.99. The specificity of the qPCR reactions was confirmed by melting curve analysis, agarose gel electrophoresis and sequencing analysis.

BGD
10, 17819–17857, 2013

2.6 Statistical analysis

Non-metric multidimensional scaling (NMDS) was used to determine the community structure similarity between samples with PRIMER (Clarke and Gorley, 2001). Bray–Curtis similarities were calculated on the OTU relative abundance matrices. The similarities were presented in a multidimensional space by plotting more similar samples closer together (Kruskal, 1964a, b). One-way analysis of similarity (ANOSIM) with 999 permutations was used to test for the significance of the differences in community composition among various NMDS clusters (Clarke, 1993). Correlations between the community structure and environmental factors were analyzed using CANOCO software (version 4.5, Microcomputer Power, USA) (Ter-Braak, 1989). The redundancy analysis (RDA) was chosen when the maximum gradient length of detrended correspondence analysis was shorter than 3.0, otherwise canonical correspondence analysis (CCA) was chosen (Lepš and Šmilauer, 2003). The environmental variables were normalized via Z transformation (Magalhães et al., 2008). Optimal CCA models were produced with automatic forward selection via Monte Carlo permutation significance tests (999 permutations). A paired or unpaired *t* test for comparison of two variables was performed using the SPSS (18.0) software package (SPSS Inc., Chicago, IL, USA).

2.7 ^{15}N incubation experiments

Nitrification and denitrification rates were measured using stable isotopic tracer methods based on Lipschultz et al. (1986). Details of the experiment procedures and calculation are described in Hsiao et al. (2013) and Hsu and Kao (2013).

Nucleotide sequence accession number

The GenBank submission numbers for the sequences from this study are KF362134-363544.

BGD
10, 17819–17857, 2013

3 Results

3.1 Biogeochemical characteristics of the region studied

Salinity ranged from 22.2 to 34.1 in April and 0.2 to 34.4 in August over our sampling sites. DO concentrations ranged from 8.3 to 11.7 and 2.6 to 8.0 mg L^{-1} in the two cruises, respectively, and were significantly lower in the bottom than the surface waters ($P = 0.000$, paired t test) and in August rather than April ($P = 0.000$, unpaired t test). The DO minimum occurred at the bottom of site YE2 in August, but did not reach the threshold of hypoxia (2 mg L^{-1}) (Renaud, 1986). TSM was measured only in August, and showed a strong gradient decreasing seaward, ranging from 2.5 to 261.8 mg L^{-1}. TSM concentrations were significantly higher in the bottom samples than those in the surface ones ($P = 0.002$, paired t test). Overall, nitrate, phosphate and silicate concentrations also revealed distinct trends, decreasing seaward. However, silicate, ranging from 2.8 to 126.6 µM, had the highest correlation ($R = 0.86$, $P < 0.0001$) with TSM. Ammonium and nitrite exhibited the biological mediated pattern, ranging from below detection limit to 1.68 µM and from 0.05 to 1.33 µM, respectively.

3.2 Phylogenetic diversity of the *amoA* and *nirS* gene clone libraries

The analysis of the *amoA* gene clone libraries was carried out only at the sites in the salinity gradient for both the April and August cruises. Nineteen β-proteobacterial and 10 archaeal *amoA* gene clone libraries were constructed successfully. β-proteobacterial *amoA* gene in three surface samples from open water with the highest salinity values was not detected, while the archaeal *amoA* gene was not detected in most of the surface samples. The analysis of the *nirS* gene clone libraries was carried out only at the sites in the salinity gradient for the April cruise, and only four libraries from the bottom samples were constructed successfully. A total of 685 β-proteobacterial and 386 archaeal *amoA* gene sequences and 338 *nirS* gene sequences were recovered. Rarefaction analyses (at 95 % DNA sequence identity) of

BGD
10, 17819–17857, 2013

each β-proteobacterial or archaeal *amoA* clone library indicated that these libraries might have encompassed the majority of the *amoA* sequence types in our sampling sites with the primers used (Fig. 2a). On the contrary, the diversity of each *nirS* clone library might have had higher *nirS* genotype diversity than recovered (Fig. 2b). The same conclusions were supported by the phylotype richness and diversity estimators (Supplement Table S1).

On the basis of phylogenetic analysis, all the β-proteobacterial *amoA* sequences fell in the *Nitrosospira* and *Nitrosomonas* clusters (Fig. 3). A total of 675 sequences from this study fell in the *Nitrosospira* cluster (571 sequences in Clade 1 and 104 sequences in Clade 2), while only 10 sequences from the closest-to-seashore site Y0 (salinity $\sim$ 0.2) in August fell in the *Nitrosomonas* cluster that is usually recovered from freshwater environments (Santoro, 2010). The sequences in Clade 1 of the *Nitrosospira* cluster had a 86 to 96 % DNA sequence identity with the sequences recovered from Baltic Sea sediments (Kim et al., 2008), and Clade 2 had a 95 to 97 % DNA sequence identity with sequences recovered from the Mediterranean sponge *Aplysina aerophoba* (Bayer et al., 2008). The *Nitrosomonas* cluster included mainly β-proteobacterial *amoA* sequences that had their closest-matched sequences recovered from Baltic Sea water (Kim et al., 2008) and *Nitrosomonas* sp. JL21. All archaeal *amoA* sequences fell in the previously described sediments (160 sequences), water column A (225 sequences), and B (one sequence) clusters (Francis et al., 2005) (Fig. 4). In general, the sequences recovered from the inshore sites with high TSM concentrations (sites Y0 and Y3 in August) fell in the Sediments cluster, except for the AugY0BP sample (the particle-associated sample from the bottom of site Y0 in August), while the sequences recovered from the sites with low TSM concentrations (site Y5 in August; sites Y3, Y4 and Y5 in April) fell in the Water column A cluster (Fig. 4).

NirS-type denitrifying bacteria are phylogenetically diverse. The phylogenetic tree grouped all *nirS* sequences into five clusters identified by Dang et al. (2009). The *nirS* sequences were predominantly (77.3 %) affiliated within Marine cluster I, and occasionally within clusters II, IV, V and VII (Fig. 5). The sequences in Marine clusters I,

BGD
10, 17819–17857, 2013

IV, V and VII had a 78 to 100 % protein sequence identity with the sequences mainly recovered from various sedimentary environments (Braker et al., 2000; Nogales et al., 2002; Liu et al., 2003; Santoro et al., 2006; Tiquia et al., 2006; Falk et al., 2007; Ruiz-Rueda et al., 2007; Dang et al., 2009; Abell et al., 2010; Mosier and Francis, 2010), while the sequences in Marine cluster II had a high protein sequence identity with the sequences recovered from estuarine and coastal sediments and waters (Nogales et al., 2002; Jayakumar et al., 2004; Castro-González et al., 2005; Hannig et al., 2006; Santoro et al., 2006). It appeared that the *nirS* sequences that we recovered from the water bottom might have originated from the YRE sediments.

3.3 Spatial structure of nitrifying and denitrifying microbial communities

Clustering analysis based on NMDS ordination and one-way ANOSIM analysis showed that there were no significance differences in community structure between AOB communities (Fig. 6a). However, AOA communities significantly separated into two or three clusters. One cluster contained communities from the inshore sites (sites Y0 and Y3 in August) with the exception of AugY0BP, which was in the other cluster containing communities from the sites with low TSM concentrations (site Y5 in August; sites Y3, Y4 and Y5 in April) (Fig. 6b). This cluster pattern was consistent with the phylogenetic analysis of the archaeal *amoA* gene. Moreover, AOA communities in the low TSM cluster further separated into the free-living and particle-associated sub-clusters. Although an obvious separation between the *nirS* clone libraries could be observed in the NMDS ordination (Fig. 6c), there were no statistically significant differences in community composition using ANOSIM analysis due to the insufficiently large sample number.

3.4 Spatio-temporal variation in *amoA* and *nirS* gene abundances

QPCR quantification was performed for all fifty samples in April and August. β-proteobacterial *amoA* gene abundance varied ranging from below detection limit (in the Y5SP, particle-associated sample from the surface of site Y5) to 1.56×10^6 copies L^{-1}

BGD
10, 17819–17857, 2013

(YE5BP, particle-associated sample from the bottom of site YE5) in August (Fig. 7) and from 5.30×10^2 (Y5SF, free-living sample from the surface of site Y5) to 1.15×10^5 copies L^{-1} (Y5BF, free-living sample from the bottom of site Y5) in April (Table 1). Archaeal *amoA* gene abundance varied ranging from 6.38×10^3 (Y3SP, particle-associated community from the surface of site Y3) to 1.72×10^8 copies L^{-1} (Y4BF, free-living community from the bottom of site Y4) in August (Fig. 7) and from below detection limit (Y3SF, free-living community from the surface of site Y3) to 6.66×10^5 copies L^{-1} (Y5BF, free-living community from the bottom of site Y5) in April (Table 1). The archaeal *amoA* gene was significantly more abundant than the β-proteobacterial *amoA* gene ($P = 0.001$, both paired and unpaired t test), suggesting that the ammonia-oxidizing process might be contributed predominantly by the archaea in the YRE. *NirS* gene abundance varied ranging from 7.54×10^3 (Y4SF, free-living community from the surface of site Y4) to 1.85×10^5 copies L^{-1} (Y3BF, free-living community from the bottom of site Y3) in April (Table 1) and from 1.59×10^4 (YE1SP, particle-associated community from the surface of site YE1) to 1.02×10^8 copies L^{-1} (Y3BP, particle-associated sample from the bottom of site Y3) in August (Fig. 7). In general, abundance of *nirS* genes was significantly lower than that of total *amoA* genes ($P = 0.001$, paired t test; $P = 0.006$, unpaired t test), suggesting that the denitrification potential was lower than that of nitrification in the region studied. All three gene abundances were significantly higher in the bottom waters than those in the surface communities ($P = 0.000$, 0.000 and 0.041 for β-proteobacterial *amoA*, archaeal *amoA* and *nirS* genes, respectively, unpaired t test), suggesting that the estuary bottom might favor the potentials for both nitrification and denitrification. Moreover, archaeal *amoA* and *nirS* gene abundances of free-living communities in August, when DO concentrations were significantly lower than those in April ($P = 0.000$, unpaired t test), outnumbered those in April ($P = 0.019$ and 0.000, respectively, unpaired t test) (Table 1).

In the salinity transect, β-proteobacterial *amoA* gene abundance generally decreased with increasing salinity in August, especially for the particle-associated samples (Fig. 7a and b). However, such a trend was not observed for the archaeal *amoA*

BGD
10, 17819–17857, 2013

gene and the highest abundance was found in the free-living community at the bottom of the offshore site Y4 in August (Fig. 7a and b; Table 1). The highest abundance of the *nirS* gene was detected in the particle-associated sample from the bottom of site Y3 in August where and when DO was lowest in this salinity transect. Notably, the abundances of particle-associated β-proteobacterial *amoA*, archaeal *amoA* and *nirS* genes were higher than the free-living ones at the closest-to-seashore site Y0 ($P < 0.05$ for each unpaired t test) and at the bottom of site Y3 ($P = 0.028$, 0.010 and 0.001, respectively, unpaired t test), where TSM concentrations were highest among all particle size-selective sampling sites. On the contrary, the three gene abundances of particle-associated samples were generally lower than the free-living ones at the most distant offshore site Y5 with the exception of the *nirS* gene in the bottom water ($P < 0.05$ for each unpaired t test) (Fig. 7a and b). The ^{15}N-based nitrification rates supported these findings (Fig. 8). In the latitude transect, however, β-proteobacterial *amoA*, archaeal *amoA* and *nirS* genes from the free-living communities, outnumbering the particle-associated ones, accounted for most cases, especially for the surface samples ($P = 0.001$, 0.001 and 0.000, respectively, unpaired t test) (Fig. 7c and d). This was consistent with the lower TSM concentrations in the latitude (2.5–60.9 mg L^{-1}) rather than the salinity transects (3.4–261.8 mg L^{-1}) ($P = 0.026$, unpaired t test).

4 Discussion

4.1 Higher potentials for both nitrification and denitrification in bottom than surface water

All *nirS* and most of the archaeal *amoA* gene sequences in this study were recovered from the bottom water using PCR and the clone library method. Moreover, qPCR quantification revealed significantly higher β-proteobacterial and archaeal *amoA* and *nirS* gene abundances in the bottom than those in the surface water. This suggested that compared to the surface water, higher potentials for both nitrification and deni-

BGD
10, 17819–17857, 2013

trification might occur in the bottom water where DO concentrations were significantly lower than those at the surface (P = 0.000, paired t test) and TSM concentrations were significantly higher (P = 0.002, paired t test). Thus, higher potentials in the bottom water might be a consequence of benefiting from environmental conditions with low DO and high TSM concentrations. Alternatively, the enhanced gene abundance was simply caused by dynamic energy due to mix/exchange of gene from sediment and water compartments, as revealed by our phylogenetic analysis. On the other hand, living phytoplankton in the surface water may compete for nutrients with nitrifiers and denitrifiers, such as ammonia and oxidized N-forms, and nitrifiers are likely photoinhibited (Merbt et al., 2012), thus resulting in low potentials for both nitrification and denitrification.

4.2 Higher potentials for both nitrification and denitrification in particle-associated rather than free-living assemblages

Although phylogenetic analysis did not show distinct differences in *amoA*-type nitrifying and *nirS*-type denitrifying microbial communities between the particle-associated and free-living assemblages, clustering analysis based on NMDS ordination suggested that AOA communities might be influenced by suspended particles since they significantly separated into the free-living and particle-associated sub-clusters in the cluster of offshore sites. Furthermore, qPCR quantification revealed significantly higher β-proteobacterial and archaeal *amoA* and *nirS* gene abundances in the particle-associated than in the free-living communities at the sites with high TSM concentrations in the river mouth, and the advantages of particle-associated over free-living samples in terms of nitrification and denitrification potentials weakened from the inner to the outer estuary. This suggested that higher potentials for both nitrification and denitrification might occur on the particles rather than in the water column. This conclusion was also supported by the significant positive correlations ($P < 0.05$) between the ratios of particle-associated vs. free-living *amoA* gene copy numbers and the ratios of ^{15}N-based nitrification rates (Fig. 8).

BGD
10, 17819–17857, 2013

We speculated that the microniche of suspended particulates could be beneficial to microbial activity. Microorganisms can take advantage of the vicinal supply of nutrients from particles (e.g., ammonia for nitrifiers; Belser, 1979). Organic particles may also serve as a direct substrate for AOA, since some *Thaumarchaeota* possess the ability to utilize amino acids heterotrophically (Ouverney and Fuhrman, 2000; Teira et al., 2006). Additionally, the lower oxygen availability in the microniche of particles was favorable for both nitrification and denitrification potentials in oxygenated water column (Kester et al., 1997). In addition, particles also offer a refuge to protect microorganisms from grazing (Tuomainen et al., 2003).

4.3 Higher nitrification than denitrification potential

Phylogenetic analysis revealed that AOA communities were dominated by Sediments and Water column A clusters of *Crenarchaeota*, whereas the *nirS* sequences were much more diverse than the *amoA* gene and closely affiliated with the sequences recovered mainly from a wide range of estuarine sediments. A similar difference between the *amoA* and *nirS* gene diversity is also reported in the study from the Fitzroy Estuary sediments in central Queensland (Abell et al., 2010). Although high levels of diversity were observed in the YRE, the *nirS* gene abundance was distinctly lower than that of total *amoA* gene in the YRE ($P = 0.006$, unpaired t test; $P = 0.001$, paired t test), suggesting lower denitrification than nitrification potential. This conclusion was supported by the ^{15}N-based nitrification and denitrification rate data. The nitrification rate strongly correlated with both β-proteobacterial and archaeal *amoA* gene abundance (Fig. 8), but the denitrification rate was below the method detection limit. Denitrifiers are reported to be often capable of several different respiratory pathways, including oxygen respiration (Santoro, 2010), and the suboxic condition with DO concentration $< 20\,\mu M$ used to separate the O_2-respiration from the NO_3^--respiration (Paulmier and Ruiz-Pino, 2009). Thus, we speculated that diverse denitrifiers were not actively conducting denitrification in the YRE water; instead, heterotrophic metabolism with O_2-respiration is more likely since DO concentrations were not low enough during our cruise periods.

BGD
10, 17819–17857, 2013

Archaeal *amoA*-type nitrifiers were suggestive of the dominant role in the ammonia-oxidizing process of the YRE, since the abundance of the archaeal *amoA* gene was significantly higher than that of the β-proteobacterial *amoA* gene ($P = 0.001$, both unpaired and paired t test). Similarly, an overwhelming dominance of AOA over AOB has been observed in various terrestrial and aquatic environments (Leininger et al., 2006; Wuchter et al., 2006; Caffrey et al., 2007; Lam et al., 2007; Mincer et al., 2007; Beman et al., 2008; Shen et al., 2008; De Corte et al., 2009; Abell et al., 2010; Beman et al., 2010; Santoro et al., 2010) with a few studies reporting a greater contribution of AOB than AOA in some estuarine environments with unlimited ammonia supply (Santoro et al., 2008; Wankel et al., 2011). Also, $^{15}NH_4^+$ oxidation rates are often reported to be intimately correlated with AOA rather than AOB *amoA* gene abundance in various marine environments (Caffrey et al., 2007; Beman et al., 2008). The dominant role played by AOA in nitrification may be due to their high affinity for ammonia (Martens-Habbena et al., 2009; Stahl and de la Torre, 2012) and thus AOA are considered to be more competitive in environments with low ammonia levels (Martens-Habbena et al., 2009), such as the water studied here (below detection limit to 1.68 µM).

4.4 Potential coupling between nitrification and denitrification

A significant positive relationship between all *amoA* and *nirS* gene abundance was observed ($P < 0.01$), which was in fact mainly contributed by the significant positive correlation of AOA *amoA* with *nirS* gene abundance ($P < 0.01$) (Fig. 9a), suggesting potential coupling between archaeal ammonia-oxidization and denitrification. The most likely place to accommodate such coupling was the microniche on suspended particle according to the significantly positive correlation between particle-associated AOA *amoA* and *nirS* gene abundance ($P < 0.01$) (Fig. 9b), which directly resulted in a good correlation between particle-associated *amoA* with *nirS* gene abundance ($P < 0.01$) as well. Although the denitrification rate was below the method detection limit throughout our survey, such gene-based coupling hinted that it would make sense once the environmental conditions permit. Although nitrification and denitrification have distinctly

BGD
10, 17819–17857, 2013

different oxygen requirements, the tight coupling between the two processes has been observed consistently by using ^{15}N incubation or gene analysis methods at the oxic–anoxic interfaces, such as the sediment–water interface, bacteria-algae mats and the oxic-anoxic transition zone of sediment or water column (Jenkins and Kemp, 1984; Rysgaard et al., 1993; Jensen et al., 1994; Risgaard-Petersen et al., 1994; Ward, 1996). Although we cannot provide concrete evidence of the biochemical linkage, we speculated that nitrifying and denitrifying processes provided directly or indirectly reactant for each other, supporting the potential coupling observed in the YRE. For example, NO_2^- produced from ammonia-oxidization might serve as a direct reactant for nitrite-reduction. Conversely, nitrite-reduction provided NO for the NO_x cycle (Schmidt et al., 2001; Kampschreur et al., 2006; Schmidt, 2008), from which N_2O_4 is produced and may potentially serve as an oxidant in ammonia-oxidization (Lund et al., 2012). Therefore, a smaller spatial distance, such as the microniche of suspended particulates, is more favorable for the two reactions to gain more reactants.

4.5 Key environmental factors revealed by statistical analysis

RDA analysis based on the *β*-proteobacterial *amoA* gene revealed that silicate concentration was the only statistically significant variable explaining the free-living AOB communities cluster pattern ($P = 0.001$), and the first axes in the RDA model explained 100 % of the cumulative variance of the bacterial *amoA*-environment relationship (Fig. 10a). In the RDA model based on the archaeal *amoA* gene, silicate and DO concentrations emerged as highly significant explanatory variables for the spatial structure of the free-living AOA communities ($P = 0.001$), and the first and second axes explained 97.4 and 2.6 % of the cumulative variance of the archaeal *amoA*-environment relationship (Fig. 10b). Silicate is reported to be one of the most common indicators discriminating river water in the ocean (Moore, 1986) and was found to have the highest correlation with TSM ($R = 0.86$, $P < 0.0001$) among all nutrients in our study area, and thus significantly contributed to formation of the spatial structure of communities in the estuary area. However, for the particle-associated AOA and AOB communities,

BGD
10, 17819–17857, 2013

no statistically significant environmental factors were obtained in CCA or RDA analysis with all available variables. We speculated that the microniche of suspended particles might be responsible for the particle-associated community structure rather than water column properties indicated by the presently investigated variables. Also, no significant environmental variables were found in the *nirS* gene-based CCA or RDA analysis, likely owing to an insufficiently large sample size (only four).

Analysis of relationships between gene abundances and environmental factors revealed a significant negative relationship between all *amoA* and *nirS* gene abundance and DO concentration ($P < 0.05$), which was in fact mainly contributed by the significant negative correlations of AOA and AOB *amoA* gene copy numbers with DO ($P < 0.01$ for each) (Fig. 11a). Furthermore, for the free-living assemblages, statistically significant negative relationships were observed between β-proteobacterial *amoA*, archaeal *amoA* or *nirS* gene abundance and DO concentration ($P < 0.01$ for each) (Fig. 11b). However, no significant relationships were found between the particle-associated gene abundances and the presently investigated variables, suggesting that the microniche of suspended particles might be responsible for the particle-associated gene distribution rather than water column properties. This speculation was further supported by the significant positive relationships between the percentage of particle-associated in total β-proteobacterial *amoA*, archaeal *amoA* or *nirS* gene abundance and TSM concentration ($P < 0.01$ for each) (Fig. 11c). It is well-known that denitrifiers favor low DO environments to conduct anaerobic respiration and AOA and AOB are highly abundant under low-oxygen conditions due to relatively high ammonia levels (Lam et al., 2007; Beman et al., 2008; Park et al., 2010; Yan et al., 2012). Our results support these consensuses. Based on the above analysis, we speculated that once DO concentration matches the stoichiometric demands of both microbial denitrification and nitrification reactions in estuary areas where organic carbon and nutrients are not limiting and where TSM concentrations are high, the coupling between nitrification and denitrification would make a significant contribution to N removal and consequently reduce the eutrophication of the YRE.

BGD
10, 17819–17857, 2013

5 Summary

This study provided the first hand dataset concerning the diversity and distribution of *amoA*-type nitrifying and *nirS*-type denitrifying microbial communities in an anthropogenically perturbed estuary with high turbidity. Our observations suggested that both nitrification and denitrification potentials were higher at the estuary bottom than in the surface water and in the particle-associated rather than the free-living assemblages of the high-turbidity river mouth. However, compared with the low diversity but high nitrification potential of *amoA*-type nitrifiers, *nirS*-type denitrifiers exhibited a rather high diversity but low denitrification potential as supported by the ^{15}N incubation experiments, suggesting that diverse denitrifiers might conduct other respiratory pathways such as oxygen respiration. Compared with the AOB, the AOA made a dominant contribution to the ammonia-oxidizing process in the YRE. Notably, potential coupling between nitrification and denitrification were revealed by the functional gene abundances, which was in fact mainly contributed by the potential coupling between denitrification and AOA ammonia-oxidization in the particle-associated assemblages. Statistical analysis revealed further that low DO and high TSM conditions favored *amoA*-type nitrifiers, *nirS*-type denitrifiers and the two processes coupling, which would significantly contribute to N removal and the reduction of eutrophication in the YRE once DO concentration matches the stoichiometric demands of both microbial denitrification and nitrification reactions.

Supplementary material related to this article is available online at http://www.biogeosciences-discuss.net/10/17819/2013/bgd-10-17819-2013-supplement.pdf.

Acknowledgements. We thank Minhan Dai, the chief scientist of the YRE project, for providing the sampling opportunity and the temperature, salinity, DO, TSM and nutrient data. We also thank Jinwen Liu, Hongjie Wang and Tao Huang for their assistance in sampling and

BGD
10, 17819–17857, 2013

sample analysis, and John Hodgkiss for his help with English. This research was funded by the MOST 973 program 2013CB955700, the NSFC projects 41176095, 91028001, 41121091 and 41023007, the NSFF project 2012J01182, the NCET project and the OPWSR project 201105021.

References

Abell, G. C. J., Revill, A. T., Smith, C., Bissett, A. P., Volkman, J. K., and Robert, S. S.: Archaeal ammonia oxidizers and *nirS*-type denitrifiers dominate sediment nitrifying and denitrifying populations in a subtropical macrotidal estuary, ISME J., 4, 286–300, 2010.

Bayer, K., Schmitt, S., and Hentschel, U.: Physiology, phylogeny and in situ evidence for bacterial and archaeal nitrifiers in the marine sponge *Aplysina aerophoba*, Environ. Microbiol., 10, 2942–2955, 2008.

Belser, L. W.: Population ecology of nitrifying bacteria, Annu. Rev. Microbiol., 33, 309–333, 1979.

Beman, J. M., Popp, B. N., and Francis, C. A.: Molecular and biogeochemical evidence for ammonia oxidation by marine *Crenarchaeota* in the Gulf of California, ISME J., 2, 429–441, 2008.

Beman, J. M., Sachdeva, R., and Fuhrman, J. A.: Population ecology of nitrifying archaea and bacteria in the Southern California Bight, Environ. Microbiol., 12, 1282–1292, 2010.

Bothe, H., Jost, G., Schloter, M., Ward, B. B., and Witzel, K.-P.: Molecular analysis of ammonia oxidation and denitrification in natural environments, FEMS Microbiol. Rev., 24, 673–690, 2000.

Braker, G., Fesefeldt, A., and Witzel, K.-P.: Development of PCR primer systems for amplification of nitrite reductase genes (*nirK* and *nirS*) to detect denitrifying bacteria in environmental samples, Appl. Environ. Microbiol., 64, 3769–3775, 1998.

Braker, G., Zhou, J., Wu, L., Devol, A. H., and Tiedje, J. M.: Nitrite reductase genes (*nirK* and *nirS*) as functional markers to investigate diversity of denitrifying bacteria in Pacific Northwest marine sediment communities, Appl. Environ. Microbiol., 66, 2096–2104, 2000.

Caffrey, J. M., Bano, N., Kalanetra, K., and Hollibaugh, J. T.: Ammonia oxidation and ammonia-oxidizing bacteria and archaea from estuaries with differing histories of hypoxia, ISME J., 1, 660–662, 2007.

BGD
10, 17819–17857, 2013

Castro- González, M., Braker, G., Farías, L., and Ulloa, O.: Communities of *nirS*-type denitrifiers in the water column of the oxygen minimum zone in the eastern South Pacific, Environ. Microbiol., 7, 1298–1306, 2005.
Clarke, K. R.: Non-parametric multivariate analyses of changes in community structure, Aust. J. Ecol., 18, 117–143, 1993.
Clarke, K. R. and Gorley, R. N.: PRIMER v5: User Manual/Tutorial, PRIMER-E, Plymouth UK, 91 pp., 2001.
Coyne, M. S., Arunakumari, A., Averill, B. A., and Tiedje, J. M.: Immunological identification and distribution of dissimilatory heme cd1 and non-heme copper nitrite reductases in denitrifying bacteria, Appl. Environ. Microbiol., 55, 2924–2931, 1989.
Dai, Z. J., Du, J. Z., Zhang, X. L., Su, N., and Li, J. F.: Variation of riverine material loads and environmental consequences on the Changjiang (Yangtze) Estuary in recent decades (1955–2008), Environ. Sci. Technol., 45, 223–227, 2011.
Dang, H., Wang, C., Li, J., Li, T., Tian, F., Jin, W., Ding, Y., and Zhang, Z.: Diversity and distribution of sediment *nirS*-encoding bacterial assemblages in response to environmental gradients in the eutrophied Jiaozhou Bay, China, Microb. Ecol., 58, 161–169, 2009.
De Corte, D., Yokokawa, T., Varela, M. M., Agogué, H., and Herndl, G. J.: Spatial distribution of bacteria and archaea and *amoA* gene copy numbers throughout the water column of the Eastern Mediterranean Sea, ISME J., 3, 147–158, 2009.
Falk, S., Hannig, M., Gliesche, C., Wardenga, R., Köster, M., Jürgens, K., and Braker, G.: *nirS*-containing denitrifier communities in the water column and sediment of the Baltic Sea, Biogeosciences, 4, 255–268, doi:10.5194/bg-4-255-2007, 2007.
Francis, C. A., Roberts, K. J., Beman, J. M., Santoro, A. E., and Oakley, B. B.: Ubiquity and diversity of ammonia-oxidizing archaea in water columns and sediments of the ocean, P. Natl. Acad. Sci. USA, 102, 14683–14688, 2005.
Hannig, M., Braker, G., Dippner, J., and Jürgens, K.: Linking denitrifier community structure and prevalent biogeochemical parameters in the pelagial of the central Baltic Proper (Baltic Sea), FEMS Microbiol. Ecol., 57, 260–271, 2006.
Hu, A., Yao, T., Jiao, N., Liu, Y., Yang, Z., and Liu, X.: Community structures of ammonia-oxidising archaea and bacteria in high-altitude lakes on the Tibetan Plateau, Freshwater Biol., 55, 2375–2390, 2010.
Hu, A., Jiao, N., and Zhang, C. L.: Community structure and function of planktonic *Crenarchaeota*: changes with depth in the South China Sea, Microb. Ecol., 62, 549–563, 2011.

BGD
10, 17819–17857, 2013

Huang, S., Chen, C., Yang, X., Wu, Q., and Zhang, R.: Distribution of typical denitrifying functional genes and diversity of the *nirS*-encoding bacterial community related to environmental characteristics of river sediments, Biogeosciences, 8, 3041–3051, doi:10.5194/bg-8-3041-2011, 2011.

Hsiao, S. S.-Y., Hsu, T.-C., Liu, J.-W., Xie, X., Zhang, Y., Lin, J., Wang, H., Yang, J.-Y. T., Hsu, S.-C., Dai, M., and Kao, S.-J.: Nitrification and its oxygen consumption along the turbid Changjiang River plume, Biogeosciences Discuss., 10, 8685–8713, doi:10.5194/bgd-10-8685-2013, 2013.

Hsu, T.-C. and Kao, S.-J.: Technical Note: Simultaneous measurement of sedimentary N_2 and N_2O production and new ^{15}N isotope pairing technique, Biogeosciences Discuss., 10, 6861–6898, doi:10.5194/bgd-10-6861-2013, 2013.

Jayakumar, D. A., Francis, C. A., Naqvi, S. W. A., and Ward, B. B.: Diversity of nitrite reductase genes (*nirS*) in the denitrifying water column of the coastal Arabian Sea, Aquat. Microb. Ecol., 34, 69–78, 2004.

Jenkins, M. C. and Kemp, W. M.: The coupling of nitrification and denitrification in two estuarine sediments, Limnol. Oceanogr., 29, 609–619, 1984.

Jensen, K., Sloth, N. P., Risgaard-Petersen, N., Rysgaard, S., and Revsbech, N. P.: Estimation of nitrification and denitrification from microprofiles of oxygen and nitrate in model sediment systems, Appl. Environ. Microbiol., 60, 2094–2100, 1994.

Kampschreur, M. J., Tan, N. C. G., Picioreanu, C., Jetten, M. S. M., Schmidt, I., and van Loosdrecht, M. C. M.: Role of nitrogen oxides in the metabolism of ammonia-oxidizing bacteria, Biochem. Soc. T., 34, 179–181, 2006.

Kester, R. A., de Boer, W., and Laanbroek, H. J.: Production of NO and N_2O by pure cultures of nitrifying and denitrifying bacteria during changes in aeration, Appl. Environ. Microbiol., 63, 3872–3877, 1997.

Kim, O.-S., Junier, P., Imhoff, J. F., and Witzel, K.-P.: Comparative analysis of ammonia monooxygenase (*amoA*) genes in the water column and sediment–water interface of two lakes and the Baltic Sea, FEMS Microbiol. Ecol., 66, 367–378, 2008.

Kruskal, J. B.: Multidimensional scaling by optimizing goodness of fit to a non-metric hypothesis, Psychometrika, 29, 1–27, 1964a.

Kruskal, J. B.: Nonmetric multidimensional scaling – a numerical method, Psychometrika, 29, 115–129, 1964b.

BGD
10, 17819–17857, 2013

Lepš, J. and Šmilauer, P.: Multivariate Analysis of Ecological Data Using CANOCO, Cambridge University Press, Cambridge, 2003.
Lam, P., Jensen, M. M., Lavik, G., McGinnis, D. F., Müller, B., Schubert, C. J., Amann, R., Thamdrup, B., and Kuypers, M. M. M.: Linking crenarchaeal and bacterial nitrification to anammox in the Black Sea, P. Natl. Acad. Sci. USA, 104, 7104–7109, 2007.
Leininger, S., Urich, T., Schloter, M., Schwark, L., Qi, J., Nicol, G. W., Prosser, J. I., Schuster, S. C., and Schleper, C.: Archaea predominate among ammonia-oxidizing prokaryotes in soils, Nature, 442, 806–809, 2006.
Lin, C. and Wu, X.: A study on characteristics of runoff amount and its important significance at the Yangtze, Nature Magazine, 21, 200–205, 1999.
Lipschultz, F., Wofsy, S. C., and Fox, L. E.: Nitrogen-metabolism of the eutrophic Delaware River ecosystem, Limnol. Oceanogr., 31, 701–716, 1986.
Liu, X., Tiquia, S. M., Holguin, G., Wu, L., Nold, S. C., Devol, A. H., Luo, K., Palumbo, A. V., Tiedje, J. M., and Zhou, J.: Molecular diversity of denitrifying genes in continental margin sediments within the oxygen-deficient zone off the Pacific coast of Mexico, Appl. Environ. Microbiol., 69, 3549–3560, 2003.
Lund, M. B., Smith, J. M., and Francis, C. A.: Diversity, abundance and expression of nitrite reductase (*nirK*)-like genes in marine thaumarchaea, ISME J., 6, 1966–1977, 2012.
Magalhães, C., Bano, N., Wiebe, W. J., Bordalo, A. A., and Hollibaugh, J. T.: Dynamics of nitrous oxide reductase genes (*nosZ*) in intertidal rocky biofilms and sediments of the Douro River Estuary (Portugal), and their relation to N-biogeochemistry, Microb. Ecol., 55, 259–269, 2008.
Martens-Habbena, W., Berube, P. M., Urakawa, H., de la Torre, J. R., and Stahl, D. A.: Ammonia oxidation kinetics determine niche separation of nitrifying archaea and bacteria, Nature, 461, 976–979, 2009.
Merbt, S. N., Stahl, D. A., Casamayor, E. O., Martí, E., Nicol, G. W., and Prosser, J. I.: Differential photoinhibition of bacterial and archaeal ammonia oxidation, FEMS Microbiol. Lett., 327, 41–46, 2012.
Mincer, T. J., Church, M. J., Taylor, L. T., Preston, C., Karl, D. M., and DeLong, E. F.: Quantitative distribution of presumptive archaeal and bacterial nitrifiers in Monterey Bay and the North Pacific Subtropical Gyre, Environ. Microbiol., 9, 1162–1175, 2007.
Moore, W. S., Sarmiento, J. L., and Key, R. M.: Tracing the Amazon component of surface Atlantic water using ^{228}Ra, salinity and silica, J. Geophys. Res., 91, 2574–2580, 1986.

BGD
10, 17819–17857, 2013

Mosier, A. C. and Francis, C. A.: Denitrifier abundance and activity across the San Francisco Bay Estuary, Env. Microbiol. Rep., 2, 667–676, 2010.
Nogales, B., Timmis, K. N., Nedwell, D. B., and Osborn, A. M.: Detection and diversity of expressed denitrification genes in estuarine sediments after reverse transcription-PCR amplification from mRNA, Appl. Environ. Microbiol., 68, 5017–5025, 2002.
Oakley, B. B., Francis, C. A., Roberts, K. J., Fuchsman, C. A., Srinivasan, S., and Staley, J. T.: Analysis of nitrite reductase (*nirK* and *nirS*) genes and cultivation reveal depauperate community of denitrifying bacteria in the Black Sea suboxic zone, Environ. Microbiol., 9, 118–130, 2007.
Ouverney, C. C. and Fuhrman, J. A.: Marine planktonic archaea take up amino acids, Appl. Environ. Microbiol., 66, 4829–4833, 2000.
Park, B.-J., Park, S.-J., Yoon, D.-N., Schouten, S., Damsté, J. S. S., and Rhee, S.-K.: Cultivation of autotrophic ammonia-oxidizing archaea from marine sediments in coculture with sulfur-oxidizing bacteria, Appl. Environ. Microbiol., 76, 7575–7587, 2010.
Paulmier, A. and Ruiz-Pino, D.: Oxygen minimum zones (OMZs) in the modern ocean, Prog. Oceanogr., 80, 113–128, 2009.
Purkhold, U., Pommerening-Röser, A., Juretschko, S., Schmid, M. C., Koops, H.- P., and Wagner, M.: Phylogeny of all recognized species of ammonia oxidizers based on comparative 16S rRNA and *amoA* sequence analysis: implications for molecular diversity surveys, Appl. Environ. Microbiol., 66, 5368–5382, 2000.
Renaud, M.: Hypoxia in Louisiana coastal waters during 1983: implications for fisheries, Fish. B-NOAA, 84, 19–26, 1986.
Risgaard-Petersen, N., Rysgaard, S., Nielsen, L. P., and Revsbech, N. P.: Diurnal variation of denitrification and nitrification in sediments colonized by benthic microphytes, Limnol. Oceanogr., 39, 573–579, 1994.
Ruiz-Rueda, O., Trias, R., Garcia-Gil, L. J., and Bañeras, L.: Diversity of the nitrite reductase gene *nirS* in the sediment of a free-water surface constructed wetland, Int. Microbiol., 10, 253–260, 2007.
Rysgaard, S., Risgaard-Petersen, N., Nielsen, L. P., and Revsbech, N. P.: Nitrification and denitrification in lake and estuarine sediments measured by the ^{15}N dilution technique and isotope pairing, Appl. Environ. Microbiol., 59, 2093–2098, 1993.

BGD
10, 17819–17857, 2013

Santoro, A. E., Boehm, A. B., and Francis, C. A.: Denitrifier community composition along a nitrate and salinity gradient in a coastal aquifer, Appl. Environ. Microbiol., 72, 2102–2109, 2006.
Santoro, A. E., Francis, C. A., de Sieyes, N. R., and Boehm, A. B.: Shifts in the relative abundance of ammonia-oxidizing bacteria and archaea across physicochemical gradients in a subterranean estuary, Environ. Microbiol., 10, 1068–1079, 2008.
Santoro, A. E.: Microbial nitrogen cycling at the saltwater–freshwater interface, Hydrogeol. J., 18, 187–202, 2010.
Santoro, A. E., Casciotti, K. L., and Francis, C. A.: Activity, abundance and diversity of nitrifying archaea and bacteria in the central California Current, Environ. Microbiol., 12, 1989–2006, 2010.
Schloss, P. D. and Handelsman, J.: Introducing DOTUR, a computer program for defining operational taxonomic units, and estimating species richness, Appl. Environ. Microbiol., 71, 1501–1506, 2005.
Schmidt, I.: Nitric oxide: interaction with the ammonia monooxygenase and regulation of metabolic activities in ammonia oxidizers, Method. Enzymol., 7, 121–135, 2008.
Schmidt, I., Bock, E., Jetten, M. S.: Ammonia oxidation by *Nitrosomonas eutropha* with NO_2 as oxidant is not inhibited by acetylene, Microbiology, 147, 2247–2253, 2001.
Seitzinger, S., Harrison, J. A., Böhlke, J. K., Bouwman, A. F., Lowrance, R., Peterson, B., Tobias, C., and Van Drecht, G.: Denitrification across landscapes and waterscapes: a synthesis, Ecol. Appl., 16, 2064–2090, 2006.
Shen, J., Zhang, L., Zhu, Y., Zhang, J., and He, J.: Abundance and composition of ammonia-oxidizing bacteria and ammonia-oxidizing archaea communities of an alkaline sandy loam, Environ. Microbiol., 10, 1601–1611, 2008.
Stahl, D. A. and de la Torre, J. R.: Physiology and diversity of ammonia-oxidizing archaea, Annu. Rev. Microbiol., 66, 83–101, 2012.
Taylor, P. G. and Townsend, A. R.: Stoichiometric control of organic carbon–nitrate relationships from soils to the sea, Nature, 464, 1178–1181, 2010.
Teira, E., Van Aken, H., Veth, C., and Herndl, G. J.: Archaeal uptake of enantiomeric amino acids in the meso- and bathypelagic waters of the North Atlantic, Limnol. Oceanogr., 51, 60–69, 2006.
Ter-Braak, C. J. F.: CANOCO – an extension of DECORANA to analyze species–environment relationships, Hydrobiologia, 184, 169–170, 1989.

BGD
10, 17819–17857, 2013

Tiquia, S. M., Masson, S. A., and Devol, A.: Vertical distribution of nitrite reductase genes (*nirS*) in continental margin sediments of the Gulf of Mexico, FEMS Microbiol. Ecol., 58, 464–475, 2006.
Tuomainen, J. M., Hietanen, S., Kuparinen, J., Martikainen, P. J., and Servomaa, K.: Baltic Sea cyanobacterial bloom contains denitrification and nitrification genes, but has negligible denitrification activity, FEMS Microbiol. Ecol., 45, 83–96, 2003.
Wang, B.: Cultural eutrophication in the Changjiang (Yangtze River) plume: history and perspective, Estuar. Coast. Shelf S., 69, 471–477, 2006.
Wang, B.: Hydromorphological mechanisms leading to hypoxia off the Changjiang Estuary, Mar. Environ. Res., 67, 53–58, 2009.
Wang, B., Wei, Q., Chen, J., and Xie, L.: Annual cycle of hypoxia off the Changjiang (Yangtze River) Estuary, Mar. Environ. Res., 77, 1–5, 2012.
Wankel, S. D., Mosier, A. C., Hansel, C. M., Paytan, A., and Francis, C. A.: Spatial variability in nitrification rates and ammonia-oxidizing microbial communities in the agriculturally impacted Elkhorn Slough Estuary, California, Appl. Environ. Microbiol., 77, 269–280, 2011.
Ward, B. B.: Nitrification and denitrification: probing the nitrogen cycle in aquatic environments, Microb. Ecol., 32, 247–261, 1996.
Wei, H., He, Y., Li, Q., Liu, Z., and Wang, H.: Summer hypoxia adjacent to the Changjiang Estuary, J. Marine Syst., 67, 292–303, 2007.
Wuchter, C., Abbas, B., Coolen, M. J. L., Herfort, L., van Bleijswijk, J., Timmers, P., Strous, M., Teira, E., Herndl, G. J., Middelburg, J. J., Schouten, S., and Damsté, J. S. S.: Archaeal nitrification in the ocean, P. Natl. Acad. Sci. USA, 103, 12317–12322, 2006.
Yan, J., Haaijer, S. C. M., Op den Camp, H. J. M., van Niftrik, L., Stahl, D. A., Könneke, M., Rush, D., Damsté, J. S. S., Hu, Y. Y., and Jetten, M. S. M.: Mimicking the oxygen minimum zones: stimulating interaction of aerobic archaeal and anaerobic bacterial ammonia oxidizers in a laboratory-scale model system, Environ. Microbiol., 14, 3146–3158, 2012.
Yan, W., Mayorga, E., Li, X., Seitzinger, S. P., and Bouwman, A. F.: Increasing anthropogenic nitrogen inputs and riverine DIN exports from the Changjiang River Basin under changing human pressures, Global Biogeochem. Cy., 24, GB0A06, doi:10.1029/2009GB003575, 2010.
Zhu, Z., Zhang, J., Wu, Y., Zhang, Y., Lin, J., and Liu, S.: Hypoxia off the Changjiang (Yangtze River) Estuary: oxygen depletion and organic matter decomposition, Mar. Chem., 125, 108–116, 2011.

BGD
10, 17819–17857, 2013

Zumft, W. G.: Cell biology and molecular basis of denitrification, Microbiol. Mol. Biol. R., 61, 533–616, 1997.

BGD
10, 17819–17857, 2013

Table 1. β-AOB and AOA *amoA* and *nirS* gene abundances from free-living communities in April and August. S: surface; B: bottom.

Samples (Salinity in Apr and Aug)	β-AOB *amoA*		AOA *amoA*		*nirS*	
	Apr	Aug	Apr	Aug	Apr	Aug
Y1S (22.2, 21.2)	$4.41 \times 10^3 \pm 6.48 \times 10^2$	$3.85 \times 10^4 \pm 3.55 \times 10^3$	$1.03 \times 10^4 \pm 5.88 \times 10^2$	$6.06 \times 10^5 \pm 4.78 \times 10^4$	$6.77 \times 10^4 \pm 7.76 \times 10^2$	$1.04 \times 10^6 \pm 8.73 \times 10^4$
Y2S (26.3, 29.0)	$8.99 \times 10^3 \pm 1.47 \times 10^3$	$9.75 \times 10^4 \pm 7.24 \times 10^3$	$3.21 \times 10^4 \pm 7.69 \times 10^3$	$5.68 \times 10^5 \pm 2.72 \times 10^5$	$5.67 \times 10^4 \pm 3.19 \times 10^3$	$1.43 \times 10^6 \pm 6.23 \times 10^4$
Y3S (30.4, 27.5)	$5.45 \times 10^2 \pm 7.76 \times 10^0$	$2.86 \times 10^3 \pm 2.78 \times 10^2$	BDL	$4.62 \times 10^5 \pm 7.96 \times 10^3$	$1.19 \times 10^4 \pm 7.07 \times 10^2$	$1.10 \times 10^5 \pm 9.37 \times 10^3$
Y4S (34.1, 28.3)	$6.38 \times 10^2 \pm 1.68 \times 10^2$	$3.56 \times 10^3 \pm 7.85 \times 10^2$	$2.67 \times 10^3 \pm 7.04 \times 10^2$	$1.74 \times 10^5 \pm 2.23 \times 10^4$	$7.54 \times 10^3 \pm 3.42 \times 10^3$	$6.63 \times 10^5 \pm 2.68 \times 10^4$
Y5S (33.9, 30.4)	$5.30 \times 10^2 \pm 1.88 \times 10^2$	$6.87 \times 10^2 \pm 7.36 \times 10^0$	$1.73 \times 10^3 \pm 7.34 \times 10^2$	$7.21 \times 10^4 \pm 3.28 \times 10^3$	$2.39 \times 10^4 \pm 2.36 \times 10^3$	$2.75 \times 10^5 \pm 3.55 \times 10^3$
Y1B (29.3, 23.1)	$5.61 \times 10^3 \pm 7.33 \times 10^1$	$3.38 \times 10^4 \pm 2.42 \times 10^3$	$2.26 \times 10^4 \pm 1.97 \times 10^3$	$9.35 \times 10^5 \pm 1.56 \times 10^4$	$6.79 \times 10^4 \pm 7.21 \times 10^3$	$1.29 \times 10^6 \pm 9.96 \times 10^4$
Y2B (30.8, 29.3)	$1.69 \times 10^4 \pm 2.53 \times 10^2$	$2.92 \times 10^4 \pm 1.39 \times 10^3$	$6.43 \times 10^4 \pm 3.11 \times 10^3$	$1.32 \times 10^6 \pm 8.41 \times 10^4$	$1.13 \times 10^5 \pm 7.25 \times 10^3$	$3.26 \times 10^5 \pm 1.33 \times 10^4$
Y3B (33.7, 30.5)	$4.22 \times 10^4 \pm 2.10 \times 10^3$	$2.20 \times 10^3 \pm 7.65 \times 10^2$	$3.75 \times 10^5 \pm 4.24 \times 10^4$	$1.06 \times 10^5 \pm 2.80 \times 10^4$	$1.85 \times 10^5 \pm 1.65 \times 10^4$	$4.15 \times 10^4 \pm 1.44 \times 10^3$
Y4B (34.1, 34.4)	$5.98 \times 10^4 \pm 2.70 \times 10^3$	$2.15 \times 10^4 \pm 6.75 \times 10^2$	ND	$1.72 \times 10^8 \pm 5.85 \times 10^6$	ND	$6.64 \times 10^5 \pm 1.30 \times 10^4$
Y5B (33.9, 34.3)	$1.15 \times 10^5 \pm 9.34 \times 10^3$	$1.55 \times 10^4 \pm 7.29 \times 10^2$	$6.66 \times 10^5 \pm 5.86 \times 10^4$	$1.43 \times 10^8 \pm 2.61 \times 10^6$	ND	$4.91 \times 10^5 \pm 3.67 \times 10^4$

BDL, below detection limit.
ND, not detected due to lack of enough environmental DNA.

BGD
10, 17819–17857, 2013

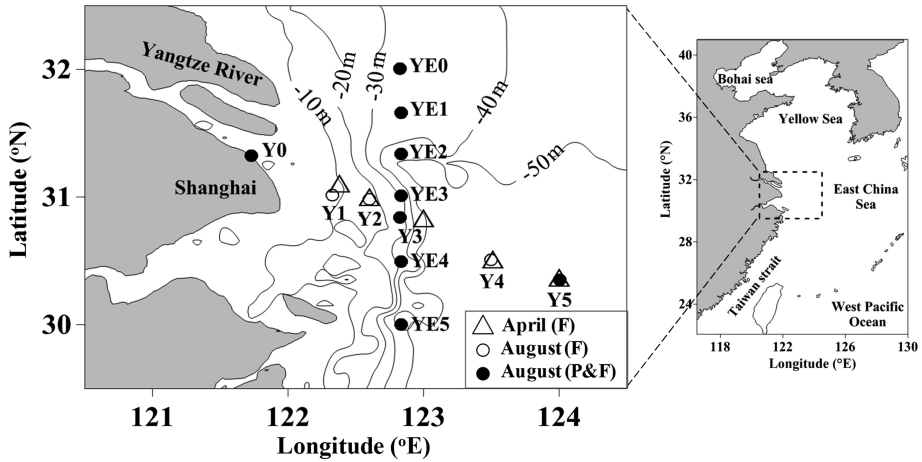

Fig. 1. Location of the study sites in the Yangtze River Estuary of the East China Sea. Isobaths are used as the background. F: free-living samples; P: particle-associated samples.

BGD
10, 17819–17857, 2013

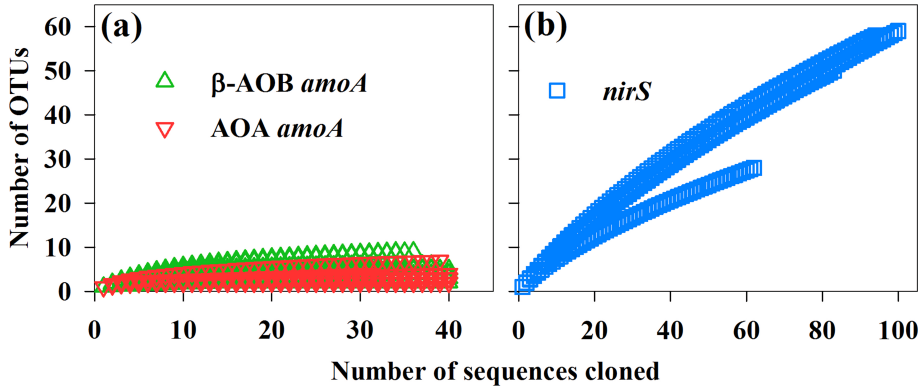

Fig. 2. Rarefaction analysis for the *β*-AOB and AOA *amoA* **(a)** and *nirS* **(b)** gene sequences. The curves were generated at 95 % DNA sequence identity.

BGD
10, 17819–17857, 2013

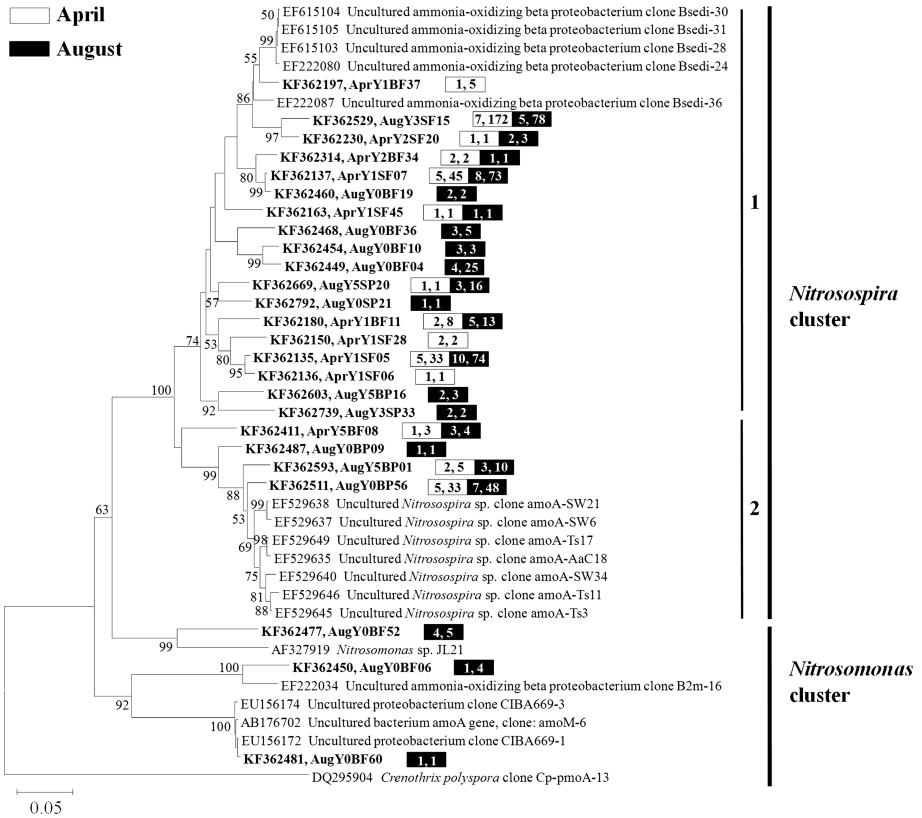

Fig. 3. Phylogenetic tree of β-AOB *amoA* constructed based on DNA sequences using the neighbor-joining method. Sequences from this study are shown in bold, and sequences sharing 95 % DNA identity are grouped. In these groups, the number of samples and sequences is shown in the frame. GenBank accession numbers are shown. Phylogenetic relationships were bootstrapped 1000 times, and bootstrap values greater than 50 % were shown. Scale bar represents the nucleotide substitution percentage.

BGD
10, 17819–17857, 2013

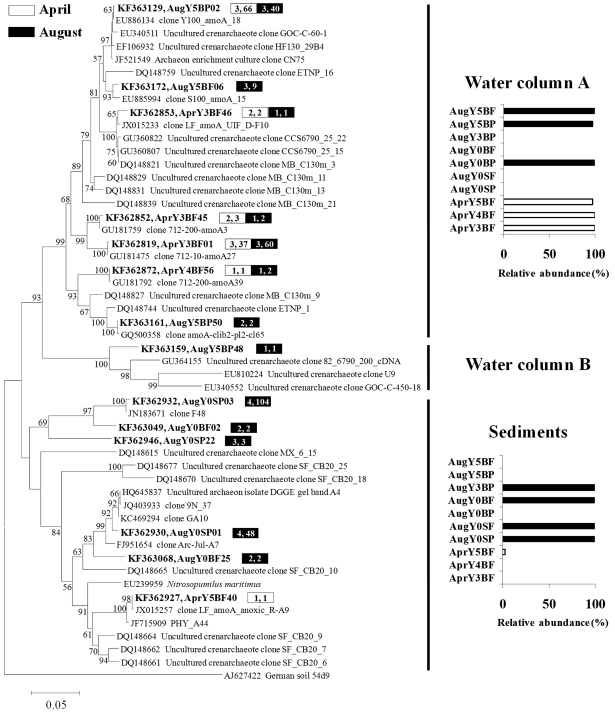

Fig. 4. Phylogenetic tree of AOA *amoA* constructed based on DNA sequences using the neighbor-joining method. Sequences from this study are shown in bold, and sequences sharing 95 % DNA identity are grouped. In these groups, the number of samples and sequences is shown in the frame. The relative abundance of clones retrieved for each clone library in the three clusters is indicated by the bar. GenBank accession numbers are shown. Phylogenetic relationships were bootstrapped 1000 times, and bootstrap values greater than 50 % were shown. Scale bar represents the nucleotide substitution percentage.

BGD
10, 17819–17857, 2013

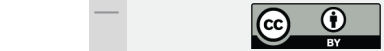

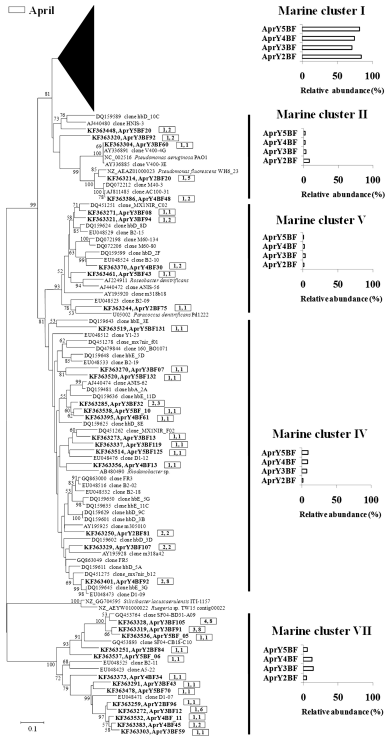

Fig. 5. Phylogenetic tree of *nirS* constructed based on amino acid sequences using the neighbor-joining method. Sequences from this study are shown in bold, and sequences sharing 95 % DNA identity are grouped. In these groups, the number of samples and sequences is shown in the frame. The relative abundance of clones retrieved for each clone library in the five clusters is indicated by the bar. GenBank accession numbers are shown. Phylogenetic relationships were bootstrapped 1000 times, and bootstrap values greater than 50 % were shown. Scale bar represents the amino acid substitution percentage.

BGD
10, 17819–17857, 2013

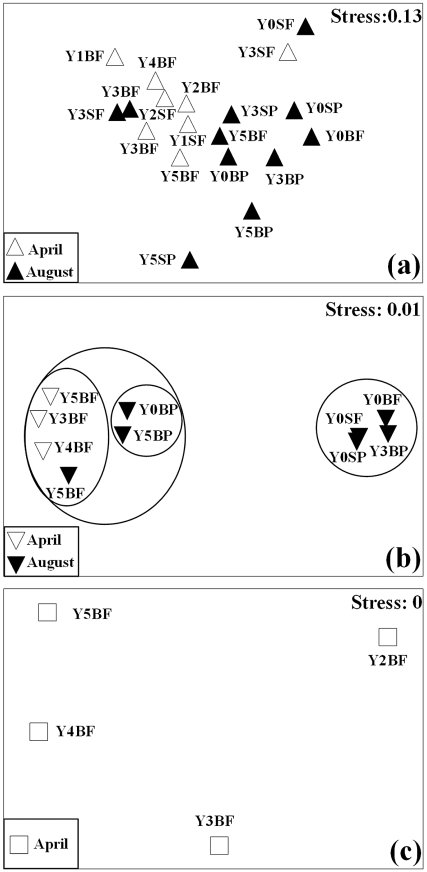

Fig. 6. NMDS ordination based on Bray-Curtis similarities between β-AOB *amoA*-type nitrifying **(a)**, AOA *amoA*-type nitrifying **(b)** or *nirS*-type denitrifying communities **(c)**. Each symbol represents an individual sample in the NMDS charts.

BGD
10, 17819–17857, 2013

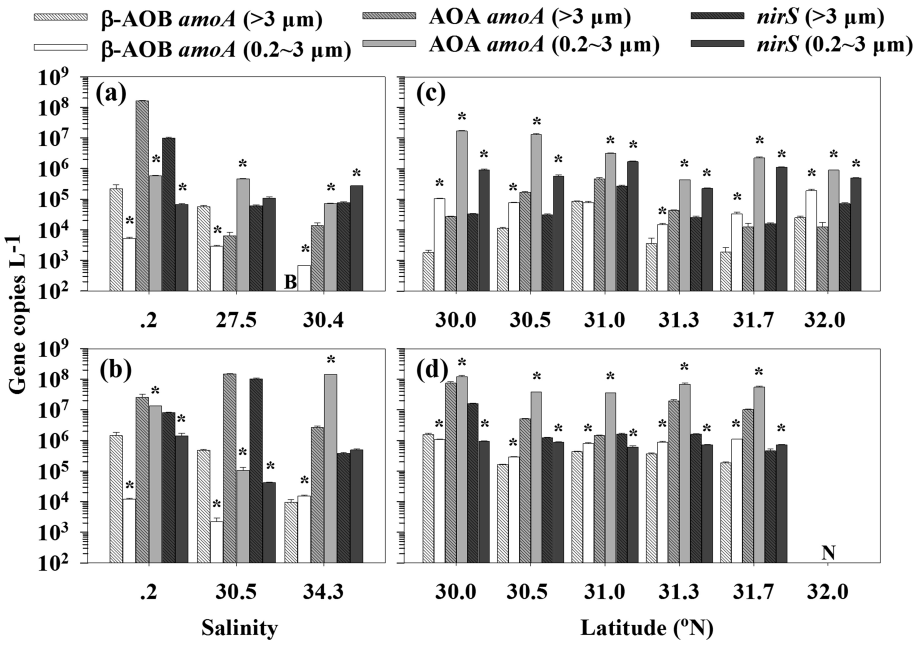

Fig. 7. *β*-AOB and AOA *amoA* and *nirS* gene abundances from the particle-associated (> 3 μm) and free-living (0.2 ~ 3 μm) communities in the salinity and latitude transects. Error bars indicate standard deviation. Asterisks indicate statistically significant differences between the particle-associated and free-living samples. **(a)** and **(b)** represent the surface and bottom samples of sites Y0, Y3 and Y5 along the salinity transect. **(c)** and **(d)** represent the surface and bottom samples of sites YE5, YE4, YE3, YE2, YE1 and YE0 along the latitude transect. B: below detection limit; N: not detected due to lack of enough environmental DNA.

BGD
10, 17819–17857, 2013

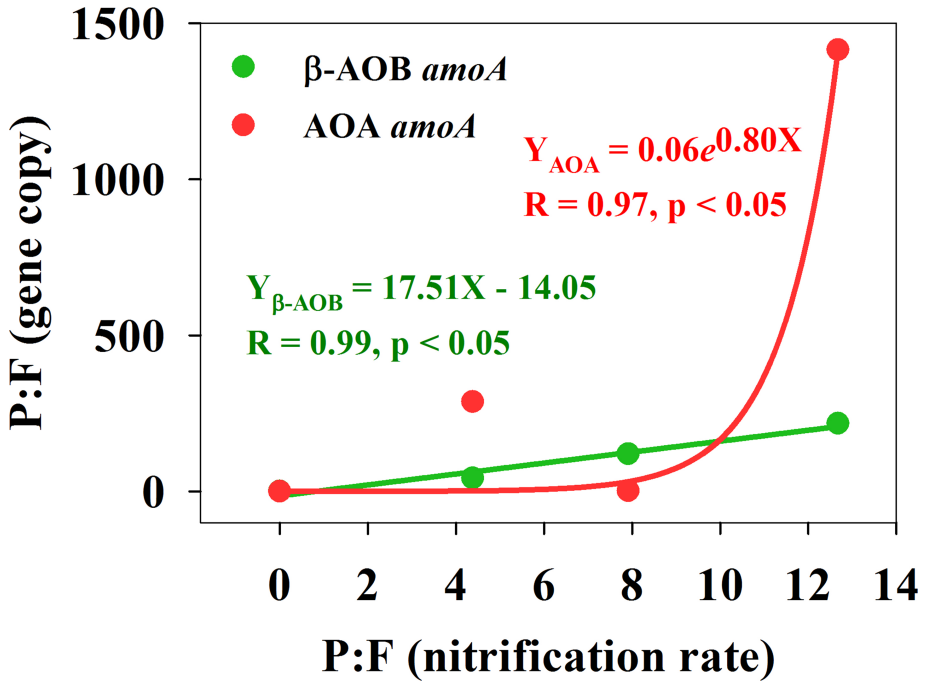

Fig. 8. Correlations between the ratios of particle-associated vs. free-living *amoA* gene copy numbers and the ratios of ^{15}N-based nitrification rates.

BGD
10, 17819–17857, 2013

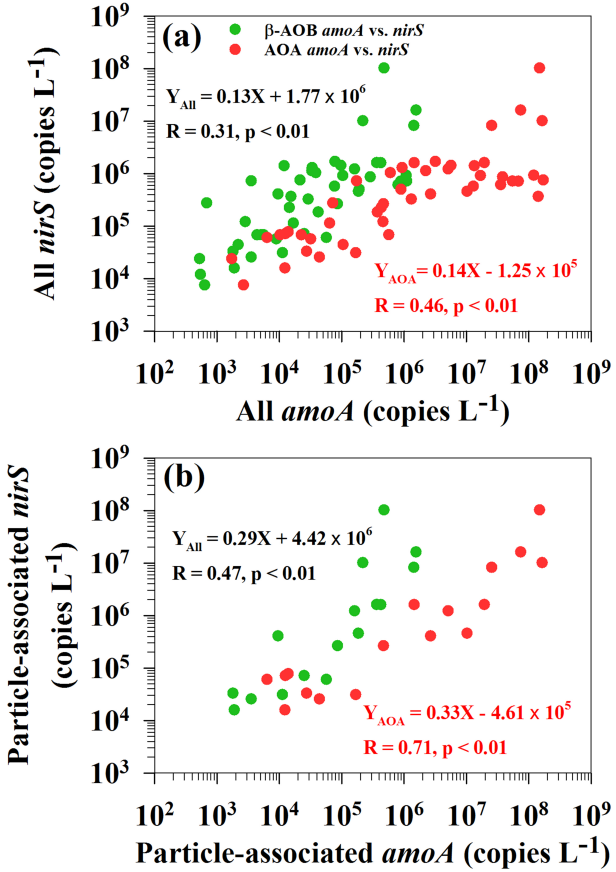

Fig. 9. Analysis of relationships between the *amoA* and *nirS* gene abundances. **(a)** all *nirS* vs. all *amoA* gene abundances; **(b)** particle-associated *nirS* vs. *amoA* gene abundances.

BGD
10, 17819–17857, 2013

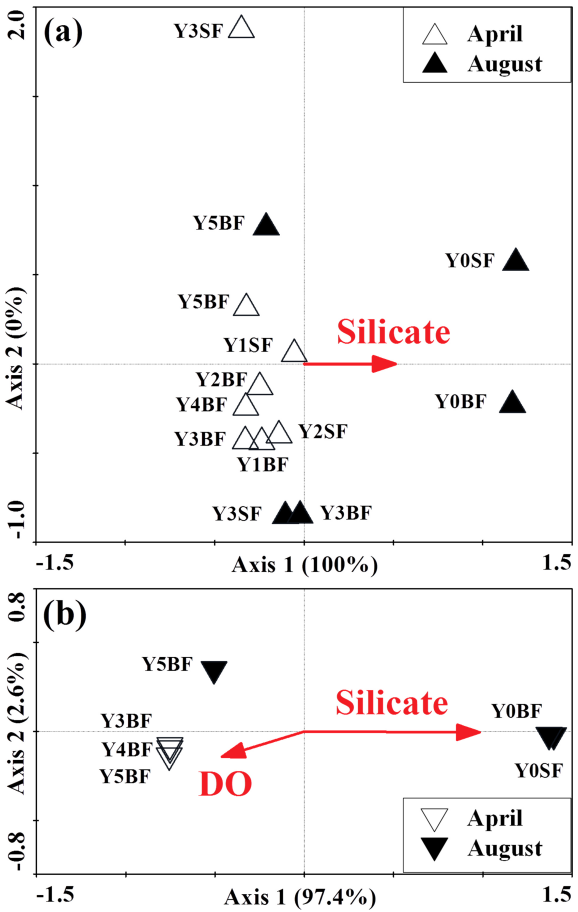

Fig. 10. RDA analysis of free-living β-AOB **(a)** and AOA *amoA*-type **(b)** nitrifying communities. Each symbol represents an individual sample. Arrows represent statistically significant environment factors explaining the observed patterns (P = 0.001). DO: dissolved oxygen.

BGD
10, 17819–17857, 2013

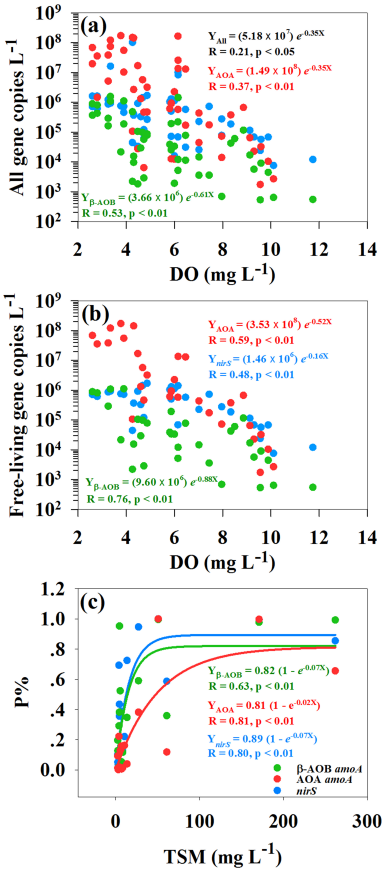

Fig. 11. Analysis of relationships between the gene abundances and environmental factors. **(a)** All *amoA* and *nirS* gene abundance vs. DO concentration; **(b)** *amoA* and *nirS* gene abundance from free-living assemblages vs. DO concentration; **(c)** percentage of particle-associated in total gene abundances vs. TSM concentration.

BGD
10, 17819–17857, 2013